$\Delta G_E^*$, to the microscopic activation free energies of eq 11 is derived from eq 3, again with use of the Eyring equation:[6,16]

$$e^{\Delta G_E^*/RT} = e^{\Delta G_{3E}^*/RT} + e^{\Delta G_{5E}^*/RT} \quad (12)$$

Equations 11 and 12 can be solved for the microscopic free energies of activation in terms of measurable quantities:

$$\Delta G_{3E}^* = \Delta G_E^* + RT \ln f_3 \quad (13)$$

$$\Delta G_{5E}^* = \Delta G_E^* + RT \ln f_5 \quad (14)$$

The activation free energy $\Delta G_E^*$ is calculted from observed values of $k_E$,[2] and values of $f_3$ and $f_5$ are available from fits of proton inventories to eq 7. Equations 13 and 14 were used to calculate the free energies of the $k_3$ and $k_5$ transition states, respectively, with respect to the free E + free A reactant state.

In the absence of MeCN, the PNPA reaction traverses successive transition states of nearly equal free energy, with the chemical transition state dominating rate determination by 400 ± 200 cal mol$^{-1}$. For the PNPP reaction (energy diagram not shown), the $k_5$ transition state dominates by 210 ± 80 cal mol$^{-1}$. For the PNPB, which has a 7.5-fold higher $V/K$ than does PNPA,[2] the chemical transition state is rate-determining. Therefore, as CEase specificity increases on extension of the acyl chain from $C_2$ (PNPA) to $C_4$ (PNPB), both the $k_3$ and $k_5$ transition states are stabilized, but with $k_3$ the primary beneficiary. Since $k_3$ is isotopically insensitive, it is reasonable to assign a substrate-triggered enzyme isomerization (induced fit[20]) to the $k_3$ step.

MeCN inhibition has different effects on the acylation dynamics of PNPA and PNPP reactions, on the one hand, and the PNPB reaction, on the other. As the free energy diagrams show, MeCN inhibition brings the $k_3$ and $k_5$ transition states of the PNPB reaction into balance by decreasing $k_3$ more than $k_5$, so that both contribute to rate determination. When the free energies of the $k_3$ and $k_5$ transition states are already balanced, as in the free energy diagrams of the PNPA reaction, MeCN has no effect on their relative energies.

**Conclusion.** As discussed in the preceding paper, there are regions of sequence similarity among CEase,[21] BuChE,[22] and AChE.[23] This structural similarity apparently has important functional consequences. Rosenberry suggested that at least for neutral ester substrates induced fit is a prominent component of the acylation reaction dynamics of AChE catalysis.[24,25] This suggestion is supported by pH-rate and solvent isotope effect investigations of AChE-catalyzed hydrolysis of anilides and esters.[4,6,7,26,27] The work described in this paper indicates that CEase utilizes a similar strategy for the generation of catalytic power. Evidently, induced fit not only poises the CEase active site for subsequent stabilization of chemical transition states but also provides the means by which the enzyme expresses substrate specificity.

**Acknowledgment.** This research was supported by NIH Grant HL30089 and by a Research Career Development Award to D.M.Q. from the National Heart, Lung and Blood Institute of NIH (HL01583, 1985-1990).

(20) Koshland, D. E., Jr. *Proc. Natl. Acad. Sci. U.S.A.* **1958**, *44*, 98-104.

(21) Kissel, J. A.; Fontaine, R. N.; Turck, C. W.; Brockman, H. L.; Hui, D. Y. *Biochim. Biophys. Acta* **1989**, *1006*, 227-236.

(22) Lockridge, O.; Bartels, C. F.; Vaughan, T. A.; Wong, C. K.; Norton, S. E.; Johnson, L. L. *J. Biol. Chem.* **1987**, *262*, 549-557.

(23) Schumacher, M.; Camp, S.; Maulet, Y.; Newton, M.; MacPhee-Quigley, K.; Taylor, S. S.; Friedmann, T.; Taylor, P. *Nature* **1986**, *319*, 407-409.

(24) Rosenberry, T. L. *Adv. Enzymol. Relat. Areas Mol. Biol.* **1975**, *43*, 103-218.

(25) Rosenberry, T. L. *Proc. Natl. Acad. Sci. U.S.A.* **1975**, *72*, 3834-3838.

(26) Quinn, D. M.; Swanson, M. L. *J. Am. Chem. Soc.* **1984**, *106*, 1883-1884.

(27) Acheson, S. A.; Dedopoulou, D.; Quinn, D. M. *J. Am. Chem. Soc.* **1987**, *109*, 239-245.

# Convergent Functional Groups. 8. Flexible Model Receptors for Adenine Derivatives

**Tjama Tjivikua, Ghislain Deslongchamps, and Julius Rebek, Jr.***

*Contribution from the Departments of Chemistry, University of Pittsburgh, Pittsburgh, Pennsylvania 15260, and The Massachusetts Institute of Technology, Cambridge, Massachusetts 02139.* *Received March 30, 1990*

**Abstract:** The energetics of complexation of highly flexible model receptors with adenine derivatives is reported. These cleftlike receptors, which are complementary to both hydrogen bonding edges of adenine, consist of two imides acylated to an alkyl chain. NMR titration studies reveal that intramolecular hydrogen bonding of these receptors can compete with the chelation of 9-ethyladenine (in $CDCl_3$), resulting in lowered association constants. This phenomenon is probed by comparing the behavior of receptors with alkyl chains of varying lengths. The binding behavior of a triimide derived from tris(2-aminoethyl)amine (tren) is also described.

## Introduction

In previous disclosures,[1,2] we have described the synthesis and binding behavior of model receptors for adenine. The synthetic receptors featured aromatic surfaces for $\pi$-stacking interactions and imide functions that provided the base pairing. The hydrogen bonding and aryl stacking components provided by these relatively rigid systems could be evaluated simultaneously. Here, we describe the new behavior that arises from the use of flexible spacer groups in structures for adenine recognition.

In searching for an ideal *chelate* for adenine, we had found that structures **1a,b** derived from a 2,7-disubstituted naphthalene spacer provided simultaneous Watson-Crick, Hoogsteen, and aromatic stacking possibilities (Scheme I). Their affinity for adenine

* To whom correspondence should be addressed at the Massachusetts Institute of Technology.

(1) Askew, B.; Ballester, P.; Buhr, C.; Jeong, K.-S.; Jones, S.; Parris, K.; Williams, K.; Rebek, J., Jr. *J. Am. Chem. Soc.* **1989**, *111*, 1082-1090. Rebek, J., Jr.; Askew, B.; Buhr, C.; Jones, S.; Nemeth, D.; Williams, K.; Ballester, P. *J. Am. Chem. Soc.* **1987**, *109*, 5033-5035. Rebek, J., Jr.; Askew, B.; Ballester, P.; Buhr, C.; Costero, A.; Jones, S.; Williams, K. *J. Am. Chem. Soc.* **1987**, *109*, 6866, 6867. Rebek, J., Jr.; Williams, K.; Parris, K.; Ballester, P.; Jeong, K.-S. *Angew. Chem., Int. Ed. Engl.* **1987**, *26*, 1244, 1245.

(2) Benzing, T.; Tjivikua, T.; Wolfe, J.; Rebeck, J., Jr. *Science* **1988**, *242*, 266, 267.

0002-7863/90/1512-8408$02.50/0 

**Scheme I**

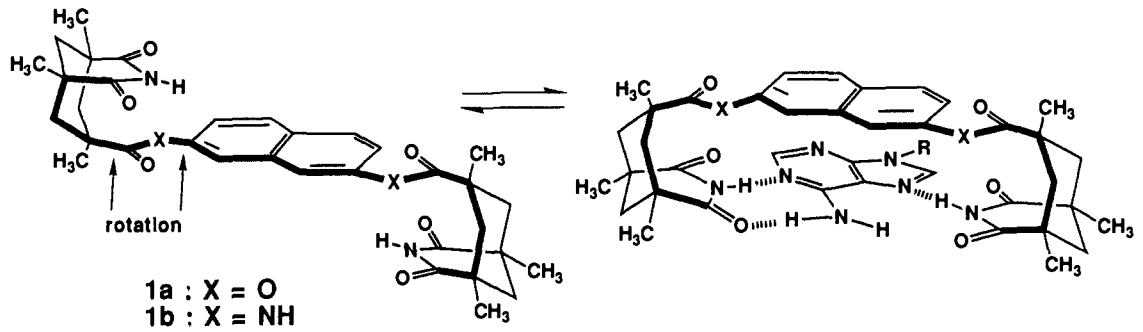


**Scheme II**

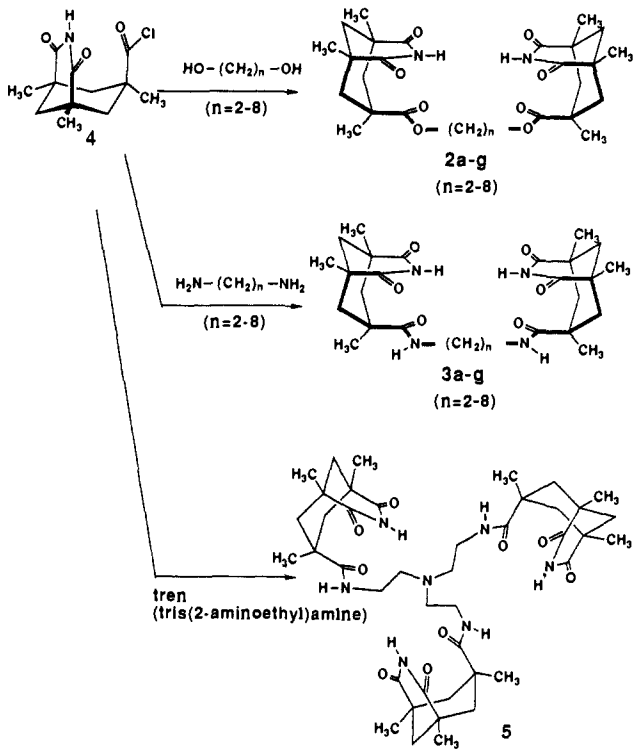


derivatives was so high that they would transport adenine and even quantities of adenosine[2] from aqueous solution into $CHCl_3$.

Molecular mechanics calculations[3] and CPK models both suggested that at least three good hydrogen bonds (ca. 2.8 Å between heavy atoms) could be achieved between substrate and synthetic receptor. The rigid aromatic spacer prevented collapse of the two imides upon each other through intramolecular hydrogen bonding. However, there was no reason to believe that naphthalene represents the optimal spacer, and we have examined some more flexible (adjustable) systems. Introducing flexibility results in entropic disadvantages for binding, since the probability of finding one particular conformer is decreased. In addition, the new spacers present complications arising from competitive intramolecular hydrogen bonding.

## Synthesis

The new structures involve the use of hydrocarbon chains as spacer elements. Their attendant rotational possibilities permit a virtual continuum of structures, and the distance between the two imide functions varies accordingly. This is in contrast to the relatively rigid aromatic systems in which the hydrogen bonding surfaces are attached through "hinges".[4] The new structures are **2a–g** and **3a–g**, which feature two imides, and **5**, in which three imides are appended to a flexible molecular framework. The compounds are prepared from condensation of the imide acid chloride **4** with the appropriate diol, diamine, or triamine (Scheme II).

(3) *MacroModel 2.5*; Still, W. C. Columbia University, 1989.
(4) For such structures see: Hamilton, A. D.; Van Engen, D. *J. Am. Chem. Soc.* **1987**, *109*, 5035, 5036. Constant, J. F.; Fahy, J.; Lhomme, J.; Anderson, J. E. *Tetrahedron Lett.* **1987**, 1777–1780.

**Table I.** Association Constants for Intramolecular Cyclization ($K_c$) and Degree of Cyclization of the Model Receptors ($CDCl_3$, 24 °C)

| entry | receptor[a] | $\nu$,[b] ppm | $K_c$[a] | cyclizn, % |
|---|---|---|---|---|
| 1 | **2a** (C2) | 9.29 | 1.7 | 63 |
| 2 | **2b** (C3) | 9.90 | 5.0 | 83 |
| 3 | **2c** (C4) | 8.36 | 0.46 | 32 |
| 4 | **2d** (C5) | 8.59 | 0.65 | 39 |
| 5 | **2e** (C6) | 7.72 | 0.11 | 10 |
| 6 | **2f** (C7) | 7.56 | 0.049 | 4.7 |
| 7 | **2g** (C8) | 7.50 | 0.028 | 2.7 |
| 8 | **3a** (C2) | 7.60 | 0.064 | 6.0 |
| 9 | **3b** (C3) | 9.75 | 3.6 | 78 |
| 10 | **3c** (C4) | 8.65 | 0.70 | 41 |
| 11 | **3d** (C5) | 8.16 | 0.33 | 25 |
| 12 | **3e** (C6) | 8.00 | 0.23 | 19 |
| 13 | **3f** (C7) | 7.70 | 0.10 | 9.0 |
| 14 | **3g** (C8) | 7.67 | 0.092 | 8.4 |
| 15 | **5** (tren) | 9.08 | 5.1[d] | 84 |

[a] Spacer chain in parentheses. [b] Chemical shift of imide N–H. [c] Based on limiting shifts of 7.42 ppm (diluted **6**) and 10.40 ppm (**2b** at −60 °C). [d] Based on limiting shifts of 7.42–9.41 ppm.

## Intramolecular Association

Some of the unusual properties of the new diimides (**2a–g**, **3a–g**) and triimide (**5**) became apparent upon their characterization by NMR spectroscopy. For example, with the aromatic derivatives such as **1**, the resonance for the N–H proton of the imide in $CDCl_3$ solution invariably occurred at 7.6 ppm. This value was taken as "free" N–H since it was observed to be concentration independent. The new structures, however, featured resonances for the imide N–H that varied between 7.5 and 9.9 ppm at room temperature (Table I).

It is significant that these values are also independent of concentration. A model system, the highly soluble cis/trans imide ester **6** was tested for its tendency to self-associate (dimerize) in $CDCl_3$.

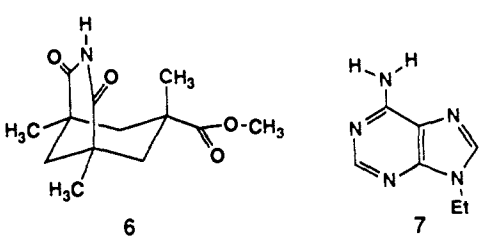

6 7

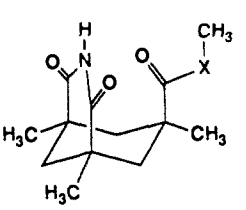

8a: X=O
8b: X=NH

**Scheme III**

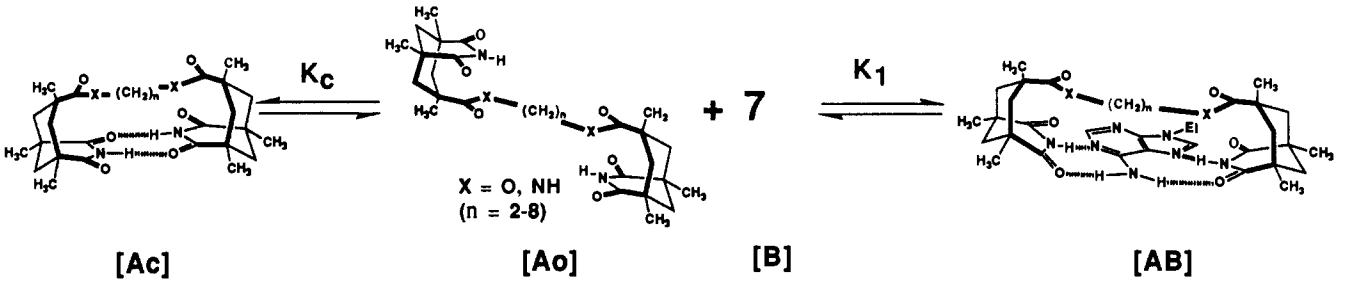


**Table II.** Association Constants and Other Parameters Observed for the Binding of 9-Ethyladenine (7) to the Model Receptors ($CDCl_3$, 24 °C)

| entry | receptor[a] | $K_c$[b] | $K_1$,[c] $M^{-1}$ | $K_a$,[d] $M^{-1}$ | $\nu$AB,[c] ppm | satn,[e] % | RMS devn[f] |
|---|---|---|---|---|---|---|---|
| 1 | **2a** (C2) | 1.7 | 112 | 41 | 12.04 | 84 | 0.015 |
| 2 | **2b** (C3) | 5.0 | 797 | 133 | 12.65 | 94 | 0.012 |
| 3 | **2c** (C4) | 0.46 | 183 | 125 | 12.10 | 91 | 0.007 |
| 4 | **2d** (C5) | 0.65 | 4810 | 2915 | 13.09 | 100 | 0.080 |
| 5 | **2e** (C6) | 0.11 | 1554 | 1400 | 12.82 | 100 | 0.097 |
| 6 | **2f** (C7) | 0.049 | 552 | 526 | 12.60 | 98 | 0.037 |
| 7 | **2g** (C8) | 0.028 | 823 | 801 | 12.73 | 99 | 0.038 |
| 8 | **3a** (C2) | 0.064 | 86 | 81 | 11.79 | 86 | 0.066 |
| 9 | **3b** (C3) | 3.6 | 173 | 38 | 12.04 | 85 | 0.004 |
| 10 | **3c** (C4) | 0.7 | 200 | 118 | 12.84 | 91 | 0.009 |
| 11 | **3d** (C5) | 0.33 | 851 | 640 | 13.41 | 97 | 0.057 |
| 12 | **3e** (C6) | 0.23 | *g* | *g* | *g* | *g* | *g* |
| 13 | **3f** (C7) | 0.10 | *g* | *g* | *g* | *g* | *g* |
| 14 | **3g** (C8) | 0.092 | 500 | 458 | 12.88 | 96 | 0.023 |
| 15 | **5** (tren) | 5.1 | 995 | 163 | 12.92 | 94 | 0.011 |

[a] Spacer chain in parentheses. [b] From Table I. [c] From nonlinear least-squares analysis. [d] Defined as $K_a = K_1/(1 + K_c)$. [e] Upon addition of 27 equiv of **7**. [f] Root-mean-square deviation of the residuals (ppm). [g] Precipitated from solution upon addition of guest.

At the highest concentration and the lowest temperature attainable, the limiting chemical shift for **6** was 9.8 ppm, a value approaching that observed for the intramolecular association of compounds **2a–g**. The values observed then represent the degree of intramolecular hydrogen bonding of the imide functions of the new synthetic receptors bearing flexible spacers (i.e., Scheme III, Ac ↔ Ao).

The chemical shifts observed for **2**, **3**, and **5** serve to define the fraction of cyclized receptor and, thus, the association constant for cyclization $K_c$ (Table I). Limiting shifts were determined by dilution of **6** (free imide ~7.42 ppm) and low-temperature (–60 °C) NMR of **2b** (cyclic imide ~10.40 ppm). The observed fraction of cyclic forms varied from 3% to about 84% at ambient temperature. Molecular mechanics calculations suggested that a three-carbon spacer is nearly optimal for producing the cyclized form without creating several unpleasant conformational problems in the hydrocarbon chain. The maximum $K_c$ was indeed observed for **2b** and **3b**. For larger spacers, a gradual decrase is observed as entropy and conformational problems conspire against cyclization.

For the tren derivative **5**, the maximum shift expected is only 9.41 ppm, since even in its cyclic form the third imide is free. The value of $K_c$ reported for **5** (5.1) must also be statistically corrected for comparison with other compounds. The intrinsic value for $K_c$ is 1.7 since there are three ways to form the cyclic system with **5** but only one way for it to dissociate.[5]

### Binding to Adenine Derivatives

The capacity for intramolecular hydrogen bonding was also expressed in the reduced affinity of these materials for 9-ethyladenine (**7**). The association constants were determined by a nonlinear least-squares fit of the titration curves to the complete equilibrium model[6] represented in Scheme III, where $K_1$ corresponds to the association constant of the "open" conformation of the host. The values for $K_c$ and $K_1$ can be translated into an "overall" association constant $K_a$, defined by the model as $K_a = K_1/(1 + K_c)$. This value ($K_c$) corresponds to the corrected association constant of the receptors, taking into account their self-association.[7]

**Scheme IV**

$$K_c = [Ac] / [Ao] \qquad [A_T] = [Ao](1+K_c) + [AB]$$

$$K_1 = [AB] / [Ao][B] \qquad [B_T] = [B] + [AB]$$

$$\nu_{obs'd} = \frac{[Ao]}{[A_T]}(\nu Ao + K_c \nu Ac) + \frac{[AB]}{[A_T]}\nu AB$$

Formation of 1:2 complexes (i.e., 1 receptor + 2 guests) was neglected in this treatment, since the structure of the 1:1 complexes generally involved some degree of chelation. The stoichiometry of these complexes was nevertheless established as 1:1 by the continuous variation method. Representative job plots for receptors **2g**, **3a**, and **5** are shown in the Experimental Section.

The equilibrium model can be described algebraically by the expressions in Scheme IV, where [At] and [Bt] stand for the total concentrations of host and guest, while [Ao], [Ac], [B], and [AB] represent the concentrations of "open" host, cyclic host, free guest, and 1:1 complex, respectively. The terms $\nu$Ao, $\nu$Ac, and $\nu$AB represent the chemical shifts of "open" host, cyclic host, and 1:1 complex, respectively, while $\nu_{obsd}$ stands for the observed chemical shift.

The association constants calculated for **2**, **3**, and **5** are reported in Table II along with limiting values of $\nu$AB.

The limiting chemical shift values for 1:1 complexes ($\nu$AB), assuming noncooperative binding sites, can be predicted as follows: With 7.42 and 13.20 ppm as reference chemical shifts for free and adenine-bound imides, we obtain 10.31 ppm for an "open" complex and 13.20 ppm for a perfectly chelated complex of hosts

(5) In fact, there are two ways to form a cyclic dimer with **2** or **3**, and six ways with **5**, but we have simplified the discussion by "normalizing" to one and three ways.

(6) Adapted from: Long, J. R.; Drago, R. S. *J. Chem. Educ.* **1982**, *59*, 1037–1039. For an application of this method to another system, see: Buchet, R.; Sandorfy, C. *J. Phys. Chem.* **1984**, *88*, 3274–3282.

(7) For a simple 1:1 model $K_a = [AB]/[A][B]$ (1). For the self-associating model [A] = [Ao] + [Ac] (2), [Ac] = $K_c$[Ao] (3), and $K_1 = [AB]/[Ao][B]$ (4). By substituting eqs 2–4 into eq 1, one obtains the following relationship: $K_a = K_1/(1 + K_c)$ (5).

Chart I

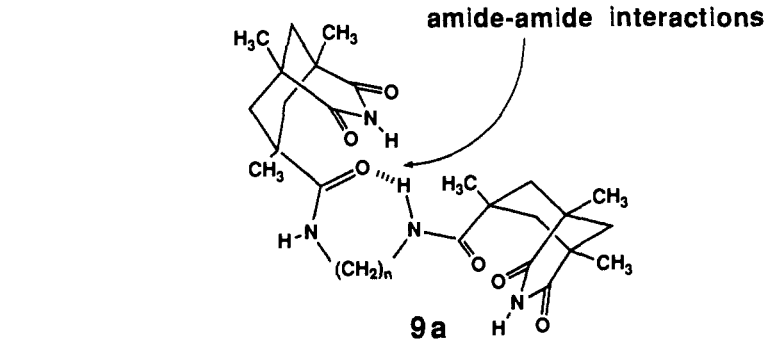


9a

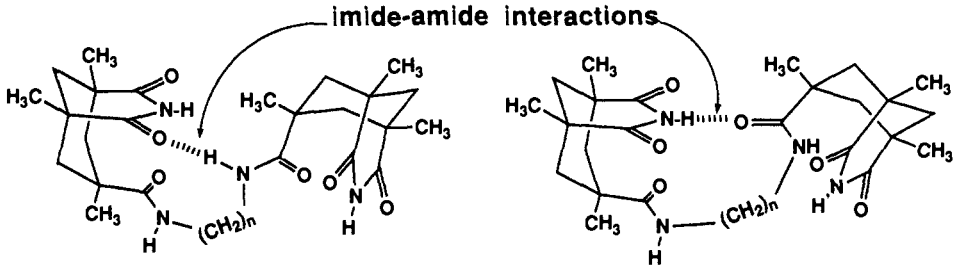


9b 9c

**2a–g** and **3a–g**. For **5**, the expected shifts are 9.35 ppm (one imide bound) and 11.27 ppm (chelate + one free imide).

Table II reveals that hosts **2a–g** (and **3a–g**) all bind **7** in a partial or completely chelated fashion, since the limiting chemical shifts of the complexes ($\nu$AB) are all greater than 10.31 ppm. The limiting shift of 12.92 ppm for the tren-derived complex of **5** also suggests chelation of adenine with additional contact with the third imide function.

**Binding Properties of Diester Diimides 2a–g**

A typical association constant for a monoimide ester (such as **8a**) in $CDCl_3$ is 45 $M^{-1}$. In the ethylene glycol derived receptor **2a**, the two imides cannot easily be brought to bear on a single adenine nucleus, and one would predict a (statistically corrected) $K_1$ of $2 \times 45 = 90$ $M^{-1}$. The observed value of 112 $M^{-1}$ suggests slight participation of the second imide function in the binding of **7**. This is also supported by the observed $\nu$AB of 12.04 ppm, which is higher than the anticipated 10.31 ppm for a nonchelated 1:1 complex. The capacity for intramolecular hydrogen bonding was also expressed by the reduced affinity of **2a** for **7** ($K_a$ = 41).

The 1,3-propane diester **2b** allows for a better chelation of the adenine nucleus, thus raising $K_1$ to 797 $M^{-1}$. This is also supported by the observation of a higher $\nu$AB (12.65 ppm). The corrected binding ability of **2b** is greatly reduced, however, reflecting the presence of the intramolecular association ($K_c$ = 5.0). In fact, the $K_a$ of receptor **2b** (133 $M^{-1}$) is only marginally higher than that expected from a nonchelated 1:1 complex (~90 $M^{-1}$).

In receptor **2c**, the additional spacer methylene interferes with optimal intramolecular hydrogen bonding, resulting in a lower $K_c$ (0.46). The corrected binding constant ($K_a$ = 125 $M^{-1}$) was not improved, however, since the homologated spacer in **2c** appears to also interfere with the chelation of **7** ($K_1$ = 183 $M^{-1}$).

Molecular modeling calculations suggested that a 1,5-pentanediol spacer would provide a diimide that is very well suited for chelation of **7** through Watson–Crick and Hoogsteen complexation.[8] As anticipated, the open conformation of receptor **2d** showed the highest affinity for **7** ($K_1$ = 4810 $M^{-1}$). The fully chelated nature of this complex was further supported by observing an ideal $\nu$AB of 13.09 ppm. Despite intramolecular association ($K_c$ = 0.65), this receptor displayed a $K_a$ of 2915 $M^{-1}$, the highest value recorded for all 12 diimide receptors in this study!

The adjustable **2d** seems to bind **7** at least as well as the naphthyl diester diimide[9] **1** ($K_a$ = 2500 $M^{-1}$; Scheme I), even without aryl stacking interactions with the guest.

Increasing the length of the spacer from five to eight carbons, we anticipated a gradual decrease in $K_c$ and $K_1$ due mainly to entropic factors. Accordingly, cyclization constants of 0.65, 0.11, 0.049, and 0.028 were recorded for receptors, **2d–g**, respectively. Titration of receptor **2e** gave a $K_1$ value of 1554 $M^{-1}$ and a corresponding $\nu$AB of 12.82 ppm, reflecting its lower chelating capacity. The homologue **2f** returned a $K_1$ of 552 $M^{-1}$ and a $\nu$AB of 12.60 ppm.

To our surprise, receptor **2g** (the $C_8$ spacer) displayed a $K_1$ of 851 $M^{-1}$, a value higher than that of its shorter **2f** counterpart. The reasons for this behavior are not clear.

**Binding Properties of Diamide Diimides 3a–g**

The diamide diimide receptors **3a–g** present two additional phenomena for consideration.

First, there exist added conformational restraints imposed by intramolecular *amide–amide* hydrogen bonds within the short spacer chains (Chart I). These can destabilize certain receptor conformations that were involved in intra- and intermolecular interactions of the diester diimide analogues **2a–g**. Second, there is the possibility of intramolecular *imide–amide* hydrogen bonding, which can affect the longer receptors (i.e., **3d–g**) and reduce their capacity for chelation of adenines. This effect is expected to be less important in the diester diimide due to the lower basicity of their ester carbonyl groups (Chart I). These phenomena were supported by NMR through deshielding of the amide N–H signal relative to that of the monoamide **8b** (5.40 ppm).

In fact, the $C_2$ diamide **3a** proved to behave quite differently from its diester counterpart **2a**. Its $K_c$ was very low compared to that of **2a** (0.064 vs 1.7!), which suggested that intramolecular amide–amide interactions prevent the approach of the two imide functions to each other. Modeling suggests that the two imides of **3a** are held apart when the two amides interact via a 7-membered-ring hydrogen bond as in **9a**. This also accounts for the

(8) Saenger, W. *Principles of Nucleic Acid Structure*; Springer-Verlag: New York, 1984; Chapter 6. Hoogsteen, K. *Acta. Crystallog.* **1963**, *16*, 907–916. For a discussion, see: Turner, D. H.; Sugimoto, N.; Kierzek, R.; Dreiker, S. D. *J. Am. Chem. Soc.* **1987**, *109*, 3783–3785 and references cited therein.

(9) Williams, K.; Askew, B.; Ballester, P.; Buhr, C.; Jeong, K.-S.; Jones, S.; Rebek, J., Jr. *J. Am. Chem. Soc.* **1989**, *111*, 1090–1094.

**Table III.** Thermodynamic Parameters Determined for the Binding of 7 to Some Model Receptors

| entry | receptor[a] | $-\Delta H_{cycl}$[b] | $-\Delta H_{complex}$[b] | $-\Delta S_{cycl}$[c] | $-\Delta S_{complex}$[c] |
|---|---|---|---|---|---|
| 1 | **3a** (C2) | *d* | 9.2 | *d* | 23.6 |
| 2 | **3b** (C3) | 4.8 | 9.7 | 13.5 | 26.7 |
| 3 | **3c** (C4) | 2.0 | 7.5 | 7.9 | 16.9 |
| 4 | **3d** (C5) | 2.5 | 11.2 | 11.3 | 26.2 |
| 5 | **3g** (C8) | *d* | 13.5 | *d* | 31.5 |

[a] Spacer chain in parentheses. [b] Units: kilocalories per mole. [c] Units: entropy units. [d] Not determined.

"near-statistical" $K_1$ value of 86 $M^{-1}$ obtained when **3a** was titrated with **7**, since the imides are unable to converge in a chelating manner. Accordingly, the amide N-H signal for receptor **3a** (6.63 ppm) appeared 1.23 ppm downfield from that of monoamide **8b**, suggesting intramolecular amide–amide interactions as in **9a**.

Amide–amide interactions also seem to play a role in the behavior of the 1,3-propanediamide **3b**, as suggested by extensive deshielding of the amide N-H signal (6.59 ppm). The observed $K_c$ and $K_1$ are significantly lower than those values recorded for diester **2b**. The resulting $K_a$ (38 $M^{-1}$) is the lowest for all the diimides studied.

Titration of receptor **3c** with **7** suggests that the two amides in this structure are too far apart for significant hydrogen bonding (in fact, the amide N-H shift observed was only 6.05 ppm). The observed values of $K_c$ (0.7 $M^{-1}$) and $K_1$ (200 $M^{-1}$) closely resemble those obtained for diester **2c** ($K_c$ = 0.46, $K_1$ = 183 $M^{-1}$).

Replacement of the ester linkers with amide linkers drastically reduced the binding properties of the 1,5-pentanediamide receptor **3d**. This diimide exhibited a $K_1$ of only 850 $M^{-1}$ (compared to 4810 $M^{-1}$ for diester **2d**) despite the formation of an ideal chelate ($\nu$AB = 13.41 ppm). Molecular modeling studies suggest that intramolecular imide–amide interactions (e.g., **9b** or **9c**) may be responsible. Indeed, the amide can form a rectilinear hydrogen bond with the opposing imide with minimal conformational strain. Moreover, there are six permutations for generating imide–amide bonding pairs. The deshielded amide N-H shift (5.97 vs 5.40 ppm) for receptor **3d** supports this hypothesis. Thus, the reduced affinity of **3d** for **7** reflects this competition for hydrogen bonds.

Receptors **3e** and **3f** precipitated as 1:1 complexes upon addition of **7**; we were thus unable to determine their association constants. The 1,8-octanediamide complex **3g** with **7** was, however, soluble in $CDCl_3$, and a $K_a$ of 458 $M^{-1}$ was observed, a value somewhat lower than that observed for **2g** ($K_a \cong$ 801 $M^{-1}$). Intramolecular imide–amide hydrogen bonding may also play a role in the reduced affinity of **3g** for **7**.

The self-association and binding of **7** was also determined at various temperatures for some of the diamides. In doing so, it was assumed that the limiting values $\nu$Ao, $\nu$Ac, and $\nu$AB were temperature independent. The thermodynamic parameters resulting from the Van't Hoff plots[10] of these studies are reported in Table III.

The largest enthalpy of intramolecular cyclization ($\Delta H_{cycl}$) is observed with the 1,3-propanediamide **3b**, and the largest (compensating) decrease in entropy is also seen with this receptor. The enthalpies of complexation minus those observed for intramolecular cyclization give a fairly consistent picture of ~5 kcal/mol for simple base pairing.

## Binding Properties of Tren Triimide 5

The tren derivative **5** also displayed some unique behavior. Titration[11] with **7** gave a $K_1$ of 995 $M^{-1}$, a value slightly higher than that of its diamide counterpart **3d**. A value based on statistical expectations would be a $K_1$ of 3 × 851 ≅ 2550 $M^{-1}$ for **5**, considering the titration results of **3d** and the fact that there are three ways of forming a chelate between **5** and **7** (leaving the third imide dangling). The experimental results strongly suggest that all three imides are involved in binding. The limiting chemical shift of 12.92 ppm is considerably higher than the value predicted (11.27 ppm) for one chelate and one free imide. A possibility is that a contact point exists between the third imide N-H and the $N_3$ position of **7**. The value for $K_1$ (995 $M^{-1}$) could then be rationalized by considering that the intrinsic cyclization constant ($K_c'$) of the third imide arm to **7** is less than 1. An estimate of $K_c'$ of 0.34 may be obtained from the $K_1$ value for **3d** (995 = (3 × 851) × $K_c'$).

## Extraction Studies

The high affinity that these materials show toward adenine derivatives encouraged liquid–liquid extraction studies. Typically, the extractions involved shaking a saturated solution of adenine or its derivatives with a $10^{-3}$ M solution of the synthetic receptor in $CDCl_3$ and assaying by NMR integration. With adenine itself, only the tren derivative **5** gave evidence of extraction. Assuming a 1:1 stoichiometry, between 80% and 100% of receptor **5** was occupied by an adenine. The C-5 diester showed no ability to extract adenine, even though it can provide simultaneous Watson–Crick and Hoogsteen base pairing. The tren derivative's success in this capacity apparently involves hydrogen bonds to the $N_3$ and $N_9$-H positions of adenine.

When adenosine and **5** were extracted as above, some 15% of the sites became occupied, and with 2′-deoxyadenosine about 10% of the sites became occupied. Thus, the tren derivative **5** is able to satisfy a large number of the adenosine hydrogen bonding sites, even to the extent that the carbohydrate domain is driven into an organic medium. The higher relative affinity for adenosine vs deoxyadenosine again suggests that additional points of contact exist between the third imide and the ribose, presumably between the 2′-hydroxyl of adenosine and the third imide in **5**. Neither cytidine nor guanosine is extracted with this receptor. Specific recognition elements must be involved in the selectivity, and it is likely that these are the hydrogen bonding patterns exposed on the adenine edges. The transport of both adenosine and 2′-deoxyadenosine across model liquid membranes with these model receptors is recorded elsewhere.[2]

One of the ultimate goals of our research concerns the development of synthetic, concave molecular agents to complement the convex surfaces of small biological targets. The degree of flexibility or rigidity that is ideal for these purposes is still a matter of debate. For example, a rigid "preorganized"[12] receptor is ideal if its geometry is perfect for complexation. If not, then some adjustability or induced fit is desirable. Here, we have shown that flexible spacers can provide excellent binding properties even with competitive intramolecular hydrogen bonds. In addition, carboxylic acids[13] can bind well to adenine derivatives; thus, the ultimate receptor for adenine is still a matter for future studies.

## Experimental Section

**General Procedures.** Mass spectra were obtained on a VG Instruments Se-20 mass spectrometer or a Varian CH-5 instrument (high resolution). IR spectra were obtained on an IBM IR/32 FTIR. $^1H$ NMR spectra were obtained on either an IBM Bruker 250- or 300-MHz or on a Varian EM 390 instrument with chemical shift values reported relative to deuterated solvents or internal tetramethylsilane. Variable-temperature spectra were taken with the variable-temperature option for the Bruker instruments. NMR-grade $CDCl_3$ was dried over 4-Å molecular sieves prior to use. Melting points were obtained on a Thomas Hoover apparatus and are uncorrected.

**Titrations.** Typically, a $10^{-3}$ M $CDCl_3$ solution of receptor was prepared, a 500-μL aliquot was transferred to a 5 mm × 8 in. NMR tube, and a spectrum was recorded. Aliquots of a $10^{-2}$ M $CDCl_3$ solution of guest (**7**) were added, and a spectrum was recorded after each addition. The chemical shift of the imide N-H signal was recorded after each addition of guest solution. The addition of guest was continued until saturation was reached. The association constant $K_1$ (and $K_a$) was then determined by nonlinear least-squares fit of the titration curve to the complete equilibrium model defined in Scheme IV. Figure 1 is a typical

(10) Barrow, G. M. *Physical Chemistry*; McGraw-Hill: New York, 1979; p 256.

(11) The titration data for **5** were fit to the same model used for the diimides **2a–g** and **3a–g**. Contrary to the diimides, triimide **5** can bind **7** with both its open and its cyclic forms. It can be shown, however, that the binding equilibria for the diimides and the triimides reduce to the same expression.

(12) Cram, D. J. *Angew. Chem., Int. Ed. Engl.* **1988**, *27*, 1009.

(13) Zimmerman, S. C.; Wu, W. *J. Am. Chem. Soc.* **1989**, *111*, 8054; Adrian, J. C., Jr.; Wilcox, C. S. *Ibid.* 8055.

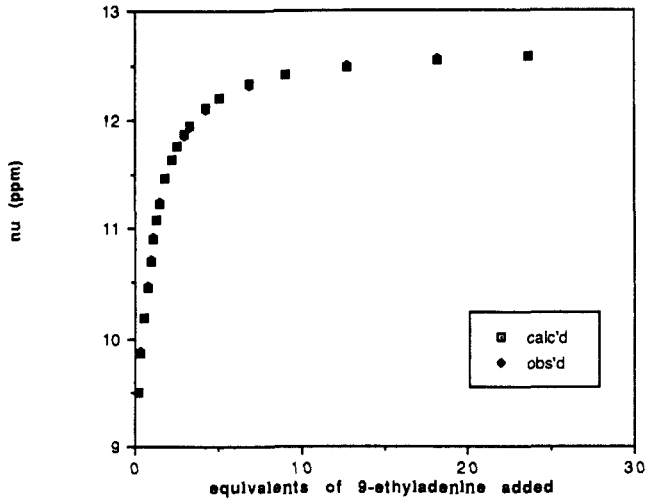


**Figure 1.** Saturation plot of tren triimide **5** + 9-ethyladenine: $K_c$ = 5.1; $K_1$ = 995; RMS deviation = 0.011.

plot of the observed and calculated titration curves obtained by this method.

**Determination of $\nu$Ac.** A $CDCl_3$ solution of receptor **2b** (showing extensive intramolecular hydrogen bonding) was analyzed by NMR by lowering the probe temperature. The temperature was lowered until no change in the chemical shift of the imide N–H was observed. The most downfield shift was taken to be representative of approximately 100% cyclic host.

**Determination of $\nu$Ao.** A dilute $CDCl_3$ solution of the monoimide **6** was prepared, and the NMR spectrum was recorded. The sample was diluted with $CDCl_3$, and the spectrum was recorded. Dilution was continued until no change in the chemical shift of the imide N–H was observed. The most upfield shift was taken to be representative of approximately 100% open host (i.e., monomeric **6**).

**Determination of Thermodynamic Parameters.** Van't Hoff plots were employed for evaluating the thermodynamics of complexation. A host/guest solution (1:1, $10^{-3}$ M) was prepared, and the chemical shift of the imide N–H signal was monitored as a function of temperature (273–333 K). From the plot of log $K_a$ as a function of temperature, the thermodynamic parameters were obtained (linear least-squares analysis).

**Extractions.** Distilled water (1 mL) was saturated with adenine or its derivatives ($\approx 10^{-3}$ M); the solution was heated and allowed to cool to room temperature. The solution was filtered through glass wool, and the filtrate was added to a 1-mL $CHCl_3$ solution of receptor ($10^{-3}$ M) in a separatory funnel. The bilayer system was shaken, and the layers were allowed to separate. The $CHCl_3$ layer was dried over $Na_2SO_4$ and evaporated under reduced pressure. The residue was vacuum-dried and dissolved in about 0.5 mL of DMSO-$d_6$ for NMR analysis.

**Determination of Stoichiometry.** A 3 mM $CDCl_3$ solution of receptor was prepared, and aliquots varying from 50 to 450 $\mu$L were transferred to NMR tubes. Aliquots of a 3 mM $CDCl_3$ solution of 9-ethyladenine were then added to complete the volumes to 500 $\mu$L. The chemical shift of the imide N–H signal was recorded for each sample, and the corresponding concentration of complex ([AB]) was determined for each.[14] Figure 2A–C shows representative Job plots for receptors **2g**, **3a**, **5** obtained by this method.

**General Procedure for the Preparation of Alkane Diester Diimides 2a–g, Alkanediamide Diimide Receptors 3a–g, and Triimide 5, Alkane Diester Diimides 2a–g.** A solution of diol **2a–g** (1 equiv), imide acid chloride[1] **4** (2.1 equiv), 4-(dimethylamino)pyridine (DMAP) (0.5 equiv), and excess $Et_3N$ in dry $CH_2Cl_2$ was heated at reflux overnight under $N_2$ atmosphere. The solution was washed with 1 N HCl and brine and dried over anhydrous $Na_2SO_4$. The crude product was subjected to flash chromatography (10:30:60 MeOH/hexanes/EtOAc on silica gel) to give pure diester diimide as a white solid.

**1,2-Ethane diester diimide 2a:** 84% yield; mp >300 °C; IR ($CHCl_3$, neat) 2957, 2929, 2871, 1728, 1693, 1462, 1286, 1123 $cm^{-1}$; $^1H$ NMR (250 MHz, $CDCl_3$) $\delta$ 9.26 (s, 2 H), 4.14 (s, 4 H), 2.71 (d, $J$ = 14.2 Hz, 4 H), 1.96 (d, $J$ = 13.3 Hz, 2 H), 1.36 (d, $J$ = 13.3 Hz, 2 H), 1.26 (s, 12 H), 1.24 (s, 6 H), 1.17 (d, $J$ = 14.2 Hz, 4 H); HRMS $m/z$ ($M^+$) calcd 504.2471, obsd 504.2469.

(14) Using the values for $K_c$, $K_1$, and $\nu$AB obtained previously, one can calculate corrected values for [AB] that take into account the receptor self-association.

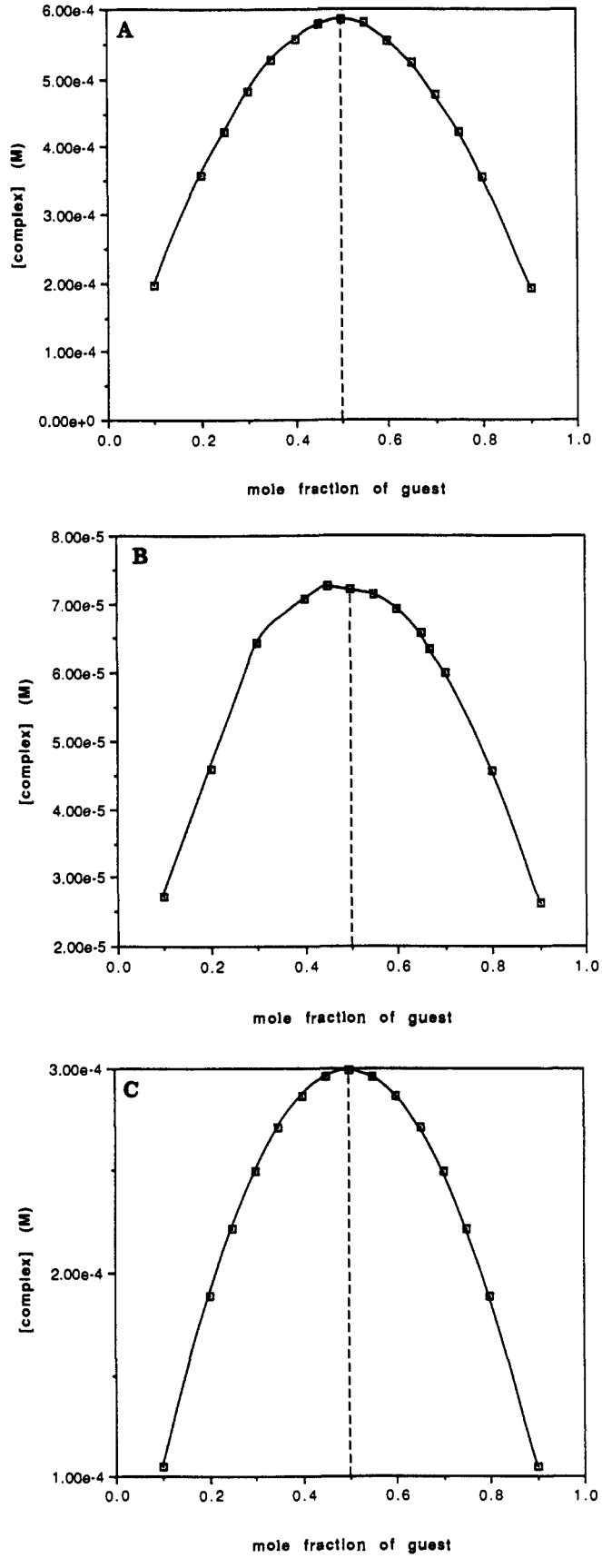


**Figure 2.** Job plot: (A) 1,8-octane diester diimide **2g** + 9-ethyladenine; (B) 1,2-ethanediamide diimide **3a** + 9-ethyladenine; (C) tren triimide **5** + 9-ethyladenine.

**1,3-Propane diester diimide 2b:** 85% yield; mp 223–225 °C; IR ($CHCl_3$, neat) 3201, 2967, 2932, 1728, 1691, 1464, 1208, 1173 $cm^{-1}$; $^1H$ NMR (250 MHz, $CDCl_3$) $\delta$ 9.90 (s, 2 H), 4.05 (t, $J$ = 6.2 Hz, 4 H), 2.70 (d, $J$ = 13.0 H, 4 H), 1.93 (d, $J$ = 12.2 Hz, 2 H), 1.37–1.12 (m, 26 H),

1.24 (s, 12 H), 1.21 (s, 6 H); HRMS $m/z$ ($M^+$) calcd 518.2628, obsd 518.2630.

**1,4-Butane diester diimide 2c**: 62% yield; mp 218–219 °C; IR ($CHCl_3$, neat) 2959, 2930, 2872, 1729, 1691, 1464, 1275, 1209, 1179 $cm^{-1}$; $^1H$ NMR (250 MHz, $CDCl_3$) $\delta$ 8.34 (s, 2 H), 4.02 (m, 4 H), 2.72 (d, $J$ = 14.2 Hz, 4 H), 1.97 (d, $J$ = 13.3 Hz, 2 H), 1.65 (m, 4 H), 1.35 (d, $J$ = 13.3 Hz, 2 H), 1.25 (s, 12 H), 1.21 (s, 6 H), 1.16 (d, $J$ = 14.2 Hz, 4 H), HRMS $m/z$ ($M^+$) calcd 532.2784, obsd 532.2785.

**1,5-Pentane diester diimide 2d**: 89% yield; mp >235 °C; IR ($CHCl_3$, neat) 3214, 2964, 2930, 1723, 1692, 1427, 1184 $cm^{-1}$; $^1H$ NMR (250 MHz, $CDCl_3$) $\delta$ 8.57 (s, 2 H), 4.01 (t, $J$ = 6.9 Hz, 4 H), 2.70 (d, $J$ = 14.2 Hz, 4 H), 1.95 (d, $J$ = 13.2 Hz, 2 H), 1.65 (m, 4 H), 1.37–1.24 (m, 4 H), 1.24 (s, 12 H), 1.21 (s, 6 H), 1.16 (d, $J$ = 14.2 Hz, 4 H); HRMS $m/z$ ($M^+$) calcd 546.2941, obsd 546.2938.

**1,6-Hexane diester diimide 2e**: 80% yield; mp 208–210 °C; IR ($CHCl_3$, neat) 3198, 2966, 2931, 1726, 1691, 1465, 1319, 1206, 1183 $cm^{-1}$; $^1H$ NMR (250 MHz, $CDCl_3$) $\delta$ 7.71 (s, 2 H), 3.99 (t, $J$ = 6.9 Hz, 4 H), 2.69 (d, $J$ = 13.5 Hz, 4 H), 1.98 (d, $J$ = 13.3 Hz, 2 H), 1.61 (m, 4 H), 1.36 (d, $J$ = 13.3 Hz, 2 H), 1.33 (m, 4 H), 1.25 (s, 12 H), 1.21 (s, 6 H), 1.16 (d, $J$ = 14.2 Hz, 4 H); HRMS $m/z$ ($M^+$) calcd 560.3097, obsd 560.3097.

**1,7-Heptane diester diimide 2f**: 94% yield; mp 200–202 °C; IR ($CHCl_3$, neat) 3210, 2965, 2932, 1727, 1696, 1462, 1316, 1206, 1184 $cm^{-1}$; $^1H$ NMR (250 MHz, $CDCl_3$) $\delta$ 7.55 (s, 2 H), 3.98 (t, $J$ = 6.9 Hz, 4 H), 2.69 (d, $J$ = 13.1 Hz, 4 H), 1.98 (d, $J$ = 13.3 Hz, 2 H), 1.58 (m, 4 H), 1.36 (d, $J$ = 13.3 Hz, 2 H), 1.30 (m, 6 H), 1.25 (s, 12 H), 1.21 (s, 6 H), 1.16 (d, $J$ = 14.2, 4 H); HRMS $m/z$ ($M^+$) calcd 574.3254, obsd 574.3252.

**1,8-Octane diester diimide 2g**: 96% yield; mp 179–181 °C; IR ($CHCl_3$, neat) 3203, 2964, 2965, 2932, 1728, 1697, 1454, 1316, 1184 $cm^{-1}$; $^1H$ NMR (250 MHz, $CDCl_3$) $\delta$ 7.50 (s, 2 H), 3.97 (t, $J$ = 7.0 Hz, 4 H), 2.69 (d, $J$ = 14.2 Hz, 4 H), 1.98 (d, $J$ = 13.2 Hz, 2 H), 1.65 (m, 4 H), 1.36 (d, $J$ = 13.4 Hz, 2 H), 1.30 (m, 8 H), 1.24 (s, 12 H), 1.21 (s, 6 H), 1.16 (d, $J$ = 14.2 Hz, 4 H); HRMS $m/z$ ($M^+$) calcd 588.3410, obsd 588.3410.

**Alkanediamide Diimide 3a–g and Triimide 5.** A solution of diamine **3a–g** or triamine **5** (1 equiv), imide acid chloride **4** (2.1 or 3.1 equiv for **5**), DMAP (0.5 equiv), and excess $Et_3N$ in dry $CH_2Cl_2$ was stirred at room temperature overnight under $N_2$ atmosphere. The solution was washed with 1 N HCl and brine and dried over anhydrous $Na_2SO_4$. The crude product was subjected to flash chromatography (10:90 MeOH/$CH_2Cl_2$ eluent on silica gel for **3a–g** and 20:80 MeOH/$CHCl_3$ eluent for **5**) to give pure product as a white solid.

**1,2-Ethanediamide diimide 3a**: 76% yield; mp >340 °C; IR (KBr) 3400, 2800, 1715, 1700, 1200 $cm^{-1}$; $^1H$ NMR (300 MHz, $CDCl_3$) $\delta$ 7.60 (s, 2 H), 6.80 (t, $J$ = 5.3 Hz, 2 H), 3.19 (q, $J$ = 7 Hz, 4 H), 2.62 (d, $J$ = 13 Hz, 4 H), 2.03 (d, $J$ = 12 Hz, 2 H), 1.43 (d, $J$ = 10 Hz, 2 H), 1.39 (d, $J$ = 12 Hz, 4 H), 1.31 (s, 6 H), 1.26 (s, 12 H); HRMS $m/z$ ($M^+$) calcd 502.2791, obsd 502.2791.

**1,3-Propanediamide diimide 3b**: 74% yield; mp 278–280 °C; IR (KBr) 3550, 2900, 1710, 1700, 1200 $cm^{-1}$; $^1H$ NMR (300 MHz, $CDCl_3$) $\delta$ 9.75 (s, 2 H), 6.21 (t, $J$ = 6 Hz, 2 H), 3.15 (q, $J$ = 7 Hz, 4 H), 2.59 (d, 14 Hz, 2 H), 1.96 (d, $J$ = 13.2 Hz, 2 H), 1.69 (m, $J$ = 7 Hz, 2 H), 1.33 (d, $J$ = 18 Hz, 2 H), 1.23 (s, 12 H), 1.20 (s, 6 H), 1.17 (d, $J$ = 15 Hz, 4 H), HRMS $m/z$ ($M^+$) calcd 516.2747, obsd 516.2948.

**1,4-Butanediamide diimide 3c**: 90% yield; mp 250–254 °C; IR (KBr), 3550, 2800, 1705, 1700, 1205 $cm^{-1}$; $^1H$ NMR (300 MHz, $CDCl_3$) $\delta$ 8.65 (s, 2 H), 5.87 (t, $J$ = 7 Hz, 2 H), 3,21 (q, $J$ = 5.4 Hz, 4 H), 2.61 (d, $J$ = 14 Hz, 4 H), 1.99 (d, $J$ = 13 Hz, 2 H), 1.48 (br m, 4 H), 1.36 (d, $J$ = 7 Hz, 2 H), ca. 1.26 (d, $J$ = 14 Hz, 2 H), 1.26 (s, 12 H), 1.21 (d, $J$ = 15 Hz, 2 H), 1.20 (s, 6 H), HRMS $m/z$ ($M^+$) calcd 530.3104, obsd 530.3106.

**1,5-Pentanediamide diimide 3d**: 79% yield; mp 202–204 °C; IR (KBr) 3000, 2900, 1715, 1700, 1200 $cm^{-1}$; $^1H$ NMR (300 MHz, $CDCl_3$) $\delta$ 8.16 (s, 2 H), 5.70 (t, $J$ = 5.3 Hz, 2 H), 3.15 (q, $J$ = 5.8 Hz, 4 H), 2.60 (d, $J$ = 14 Hz, 4 H), 1.97 (d, $J$ = 13 Hz, 2 H), 1.46 (m, $J$ = 7 Hz, 4 H), 1.35 (q, $J$ = 13 Hz, 2 H), 1.27 (m, $J$ = 14 Hz, 4 H), 1.24 (s, 12 H), 1.19 (d, $J$ = 13 Hz, 4 H), 1.18 (s, 6 H); HRMS $m/z$ ($M^+$) calcd 544.3261, obsd 544.3262.

**1,6-Hexanediamide diimide 3e**: 71% yield; mp 227–230 °C; IR (KBr) 3000, 2900, 1715, 1700, 1200 $cm^{-1}$; $^1H$ NMR (300 MHz, $CDCl_3$) $\delta$ 8.16 (s, 2 H), 5.70 (t, $J$ = 6.2 Hz, 2 H), 3.17 (q, $J$ = 6.3 Hz, 4 H), 2.59 (d, $J$ = 14 Hz, 4 H), 1.98 (d, $J$ = 13 Hz, 2 H), 1.45 (m, $J$ = 6 Hz, 8 H), 1.36 (d, $J$ = 13 Hz, 2 H), ca. 1.25 (br, 4 H), 1.25 (s, 12 H), 1.19 (s, 6 H), HRMS $m/z$ ($M^+$) calcd 558.3417, obsd 558.3417.

**1,7-Heptanediamide diimide 3f**: 83% yield; mp 227–230 °C; IR (KBr) 3300, 2900, 1705, 1700, 1190 $cm^{-1}$; $^1H$ NMR (300 MHz, $CDCl_3$) $\delta$ 7.70 (s, 2 H), 5.73 (t, $J$ = 7 Hz, 2 H), 3.14 (q, $J$ = 7 Hz, 4 H), 2.54 (d, $J$ = 14 Hz, 4 H), 2.00 (d, $J$ = 13 Hz, 2 H), 1.44 (m, $J$ = 6 Hz, 10 H), 1.37 (d, $J$ = 13 Hz, 2 H), ca. 1.27 (br d, 4 H), 1.27 (s, 12 H), 1.20 (s, 6 H); HRMS $m/z$ ($M^+$) calcd 572.3574, obsd 572.3575.

**1,8-Octanediamide diimide 3g**: 86% yield; mp 213–215 °C; IR (KBr) 3300, 2900, 1705, 1200 $cm^{-1}$; $^1H$ NMR (300 MHz, $CDCl_3$) $\delta$ 7.67 (s, 2 H), 5.73 (t, $J$ = 7.6 Hz, 2 H), 3.14 (q, $J$ = 7 Hz, 4 H), 2.56 (d, $J$ = 14 Hz, 4 H), 2.00 (d, $J$ = 13 Hz, 2 H), 1.44 (m, $J$ = 10 Hz, 12 H), 1.38 (d, $J$ = 13 Hz, 2 H), ca. 1.27 (br, 4 H), 1.27 (s, 12 H), 1.20 (s, 6 H); HRMS $m/z$ ($M^+$) calcd 586.3730, obsd 586.3730.

**Tren triamide triimide 5**: 86% yield; mp 140–163 °C; IR (KBr) 3300, 2890, 1710, 1700, 1200 $cm^{-1}$; $^1H$ NMR (300 MHz, $CDCl_3$) $\delta$ 9.05 (s, 3 H), 6.40 (br t, 3 H), 3.70 (br q, 6 H), 3.20 (br q, 6 H), 2.60 (d, $J$ = 12.7 Hz, 6 H), 1.98 (d, $J$ = 13 Hz, 3 H), 1.40 (d, $J$ = 10 Hz, 3 H), 1.36 (d, $J$ = 10 Hz, 6 H), 1.28 (s, 9 H), 1.22 (s, 18 H), HRMS $m/z$ ($M^+$) calcd 809.4687, obsd 558.3293 ($M^+$, imide arm).

**Acknowledgment.** We acknowledge financial support from the National Science Foundation. G.D. expresses his gratitude to the National Sciences and Engineering Research Council of Canada for a postdoctoral fellowship.